27Al quadrupole interaction in zeolites loaded with probe molecules - a quantum-chemical study of trends in electric field gradients and chemical bonds in clusters

ELSEVIER

Solid State Nuclear Magnetic Resonance 9 (1997) 165–175

SOLID STATE
Nuclear Magnetic
Resonance

^{27}Al quadrupole interaction in zeolites loaded with probe molecules—a quantum-chemical study of trends in electric field gradients and chemical bonds in clusters [1]

Hubert Koller, Eric L. Meijer, Rutger A. van Santen *

Laboratory of Inorganic Chemistry and Catalysis, Eindhoven University of Technology, P.O. Box 513, Eindhoven 5600 MB, Netherlands

Received 31 October 1996

Abstract

The electric field gradient (EFG) has been calculated in zeolite clusters at the aluminium site surrounded by four SiO_4 tetrahedra. Density functional theory (DFT) with the 6-31G** basis set has been employed. Formation of a Brønsted acid site by protonation of one oxygen atom of the AlO_4 tetrahedron perturbs the coordination of aluminium, i.e., the corresponding Al–O bond is considerably weaker than in the unprotonated case. This leads to a large EFG, and the calculated quadrupole coupling constant (QCC) for ^{27}Al is 18.2 MHz. Different probe molecules were adsorbed on the Brønsted site. The hydrogen bond formed between the acid proton and the probe molecule weakens the zeolitic O–H bond. For conservation of the overall bond order of the oxygen atom, its bonds to the neighboring tetrahedral atoms (Si, Al) become stronger. As a consequence, the perturbation of the AlO_4 tetrahedron and the EFG at the aluminium position decrease depending on the strength of the hydrogen bond. Perturbation of an oxygen atom of the AlO_4 tetrahedron by accepting a hydrogen bond from the base molecule also affects the corresponding Al–O bond order. A linear correlation is found between the calculated QCC constants for ^{27}Al and the Al–O bond orders of the oxygen atoms which are perturbed by protonation or by hydrogen bonds. A geometrical shear strain parameter and a simple electrostatic point charge model are less successful at predicting the trends in EFG which clearly shows the importance of the chemical bonds. Published by Elsevier Science B.V.

Keywords: ^{27}Al NMR; Calculation of electric field gradients; Density functional theory; Zeolites; Acid sites

1. Introduction

By insertion of trivalent elements into tetrahedral silicate frameworks, a negative charge is formed which is exactly balanced by extra-framework cations. The microporous members of the family of tectoaluminosilicates (zeolites) provide a pool of highly active solid acids, if charge balance for aluminium is accomplished by protons connected to framework oxygen atoms [1–4].

A detailed knowledge of the local structure and bonding at the acid site is essential in order to understand the complex catalytic function of zeolites. While the O–H bond properties of the Brønsted acid sites in dehydrated zeolites have been intensively studied, e.g., by ^{1}H NMR and infrared spectroscopies, the local aluminium environment has been

* Corresponding author. Tel.: +31-40-247-3082; fax: +31-40-245-5054.

[1] Dedicated to Günter Engelhardt on the occasion of his 60th birthday.

0926-2040/97/$17.00 Published by Elsevier Science B.V.
PII S0926-2040(97)00056-8

explored far less by experimental methods. The exact local structure is difficult to obtain by X-ray or neutron diffraction for several reasons including Si–Al disorder. The properties of the ^{27}Al nucleus in solid-state NMR spectroscopy offer a potentially sensitive means to probe the local structure.

The first ^{27}Al NMR spectrum of a zeolite in the catalytically active, dehydrated form was published by Ernst, Freude and Wolf [5], who measured the ^{27}Al NMR spectrum of zeolites ZSM-5 and Y using a static echo method. The observed signal is very broad due to a large quadrupole interaction (quadrupole moment of ^{27}Al: $Q = 0.14.10^{-28}$ m^2). Dehydrated zeolites in their catalytically active H-forms exhibit the largest quadrupole coupling constants for ^{27}Al known so far (11–18 MHz) [5–8]. These large values indicate very unusual geometric and/or electronic properties of the acid sites, that is to say the AlO_4 tetrahedra must be severely distorted. The quadrupole interaction decreases considerably when probe molecules are adsorbed [9,6], thus, reducing the distortion.

A structural interpretation of these values and trends is still lacking. Engelhardt and Veeman [10] have applied quite successfully a shear strain parameter (Ψ) for several minerals and for the microporous molecular sieve VPI-5. However, none of these solids do contain acid sites. The shear strain parameter was introduced earlier by Ghose and Tsang [11], and it will be further expounded in Section 2 (model III).

To date, the only means of obtaining suitable information about the local structure of acid sites are quantum-chemical cluster calculations [12,13]. The aim of this work was to calculate electric field gradients (EFG) for ^{27}Al in zeolite clusters interacting with probe molecules using density functional theory (DFT). Principles and trends are sought after which allow a better understanding of ^{27}Al NMR QCC for tetrahedral framework aluminium sites in zeolites.

2. Theory and clusters

The non-spherically symmetric part of the EFG is expressed by a traceless, second rank tensor with the principal components $|V_{xx}| \leq |V_{yy}| \leq |V_{zz}|$. The following definitions apply [14] for the QCC and the asymmetry parameter of the EFG (η):

$$\mathrm{QCC} = \frac{e^2 q \cdot Q}{h}, \; eq = V_{zz} \tag{1}$$

$$\eta = \frac{|V_{xx} - V_{yy}|}{|V_{zz}|} \tag{2}$$

where e is the electron charge, Q is the nuclear electric quadrupole moment, and h is the Planck constant.

For an exact electrostatic calculation of $V_{\alpha\alpha}$ ($\alpha = x, y, z$), the whereabouts of all charge-carriers are needed in a given structure. This condition is fulfilled for nuclei by the atomic coordinates, but it is particularly non-trivial for the electrons. For this reason, often simplified charge models are employed, or empirical correlations as with the aforementioned shear strain parameter are useful aids. Here, three models (i–iii) are tested for an interpretation of the QCC of ^{27}Al in zeolites.

2.1. Model I

In principle, the most exact approach is a quantum-chemical computation of EFG, which is also the most demanding method. A general problem of quantum-chemical EFG calculations is the choice of the basis set, and in most cases it is not possible to obtain EFG values that are converged with respect to the size of the basis set [15,16]. This basis set problem has also been observed for ^{27}Al [17]. Bearing in mind this drawback when using quantum-chemical calculations in model I, we were aiming for reliable geometries and relative trends of the EFG rather than correct absolute values. The soundness and usefulness of this utilitarian approach will be discussed in Section 3.

All calculations were performed with the GAUSSIAN92/DFT code [18] employing the DFT [19], and the results presented here were obtained with the 6-31G** basis set. Exchange and correlation energies were taken into account self-consistently with the hybrid method Becke3LYP in the Gaussian92/DFT program. The latter consists of Becke's three parameter exchange functional and the correlation functional of Lee, Yang, and Parr, which includes both local and non-local terms.

A portion including five tetrahedral atoms was extracted from the crystal structure of zeolite H–Y [20], and the termini were saturated with hydrogen atoms (Fig. 1). The atomic numbering in Fig. 1 is introduced here and does not correspond to Ref. [20]. The Brønsted proton selected for this study directs into the large cage (supercage) of zeolite Y. Its accessibility in the large pores makes this site catalytically relevant.

Self-consistent field optimization of the structure was carried out by lowering total cluster energies: after having optimized all bond distances, the coordinates of the hydrogen atoms on the termini and the silicon atoms were fixed. The other atomic coordinates were then varied until the change in the total cluster energy between two optimization steps was at least below a threshold of 0.2 kJ/mol. Geometric parameters directly associated with the acid site and EFG components became stable earlier than this energetic break-off-condition was achieved. The deprotonated structure and clusters with probe molecules were optimized under the same constraints as described above.

Electrostatic properties were calculated with the PRISM algorithm as implemented in the GAUSSIAN92/DFT software [21]. The electrostatic potential is deduced from two summations over nuclear and electronic contributions [21]

$$V(r) = \sum_{A} \frac{Z_A}{|r - R_A|} - \sum_{\mu\nu} P_{\mu\nu} \int \frac{\phi_\mu(r_1)\phi_\nu(r_1)}{|r - r_1|} dr \tag{3}$$

where Z_A is the nuclear charge of atom A centered at R_A, ϕ_μ and ϕ_ν are orbital basis functions, and $P_{\mu\nu}$ are elements of the density matrix. The diagonalized EFG tensor $V_{\alpha\alpha}$ ($\alpha = x, y, z$) is the second derivative of the electrostatic potential. The QCC of ^{27}Al (in MHz) is obtained from V_{zz} (in au) by QCC = $-34.9647\ V_{zz}\ Q$ [22].

2.2. Model II

A practical, yet in many cases oversimplified, possibility is to assign all charges to ionic centers and carry out a simple summation of point charge contributions to electrostatic properties. In principle, this method is a simplification of Eq. (3): the second term is eliminated and summation of the first term now runs over ionic instead of nuclear charges, bearing in mind that the second derivative of spatial components of the electrostatic potential applies for the EFG tensor. This point charge model ignores

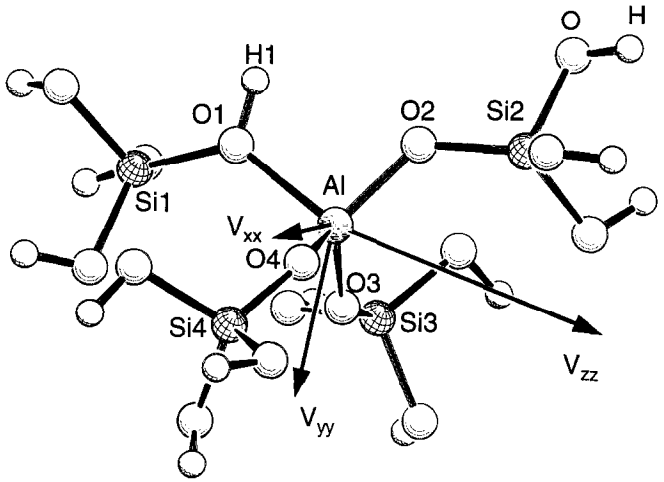

Fig. 1. Final geometry of the zeolite cluster HZ.

electronic contributions to the EFG in chemical bonds and has proven useful for ionic bonding situations like sodium cations in a series of mainly inorganic compounds including sodium silicates [23]. A simple PC program [23] was used to carry out these calculations using geometries and ionic charges as obtained by Mulliken analysis after the DFT calculations in model I. In order to take into account distortions of core electrons of aluminium due to EFG, a Sternheimer correction of 2.236 was applied for ^{27}Al [14].

2.3. Model III

The deviation from ideal tetrahedral coordination of the aluminium atom is parameterized by the so-called shear strain parameter (Ψ) which correlates

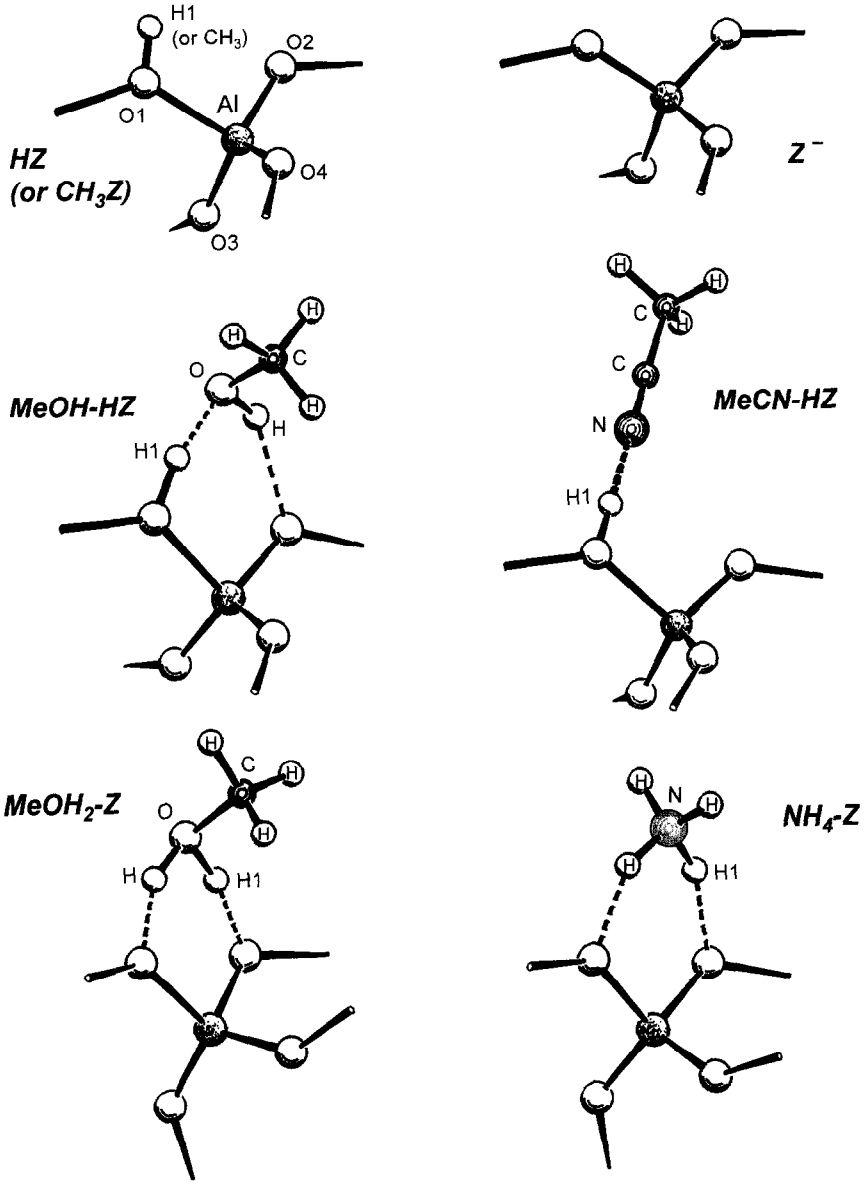

Fig. 2. Overview of the central parts of the calculated clusters.

empirically with experimental QCC [10,11]. Ψ is defined as

$$\Psi = \sum_{i=1}^{6} |\tan(\alpha_i - \alpha_0)| \quad (4)$$

where α_i is an O–Al–O angle as obtained by model I, and α_0 is the tetrahedral angle (109.5°). The Ψ values are translated into ^{27}Al QCC by using the linear correlation published by Engelhardt and Veeman [10].

2.4. Zeolite clusters

The acid–base interactions of sorbates with zeolites are studied by comparing the following clusters (see Figs. 1 and 2): the protonated zeolite cluster shown in Fig. 1 (from now on designated as HZ), the deprotonated cluster in Fig. 2 (Z^-), a protonated cluster interacting with methanol (MeOH–HZ), a protonated zeolite interacting with acetonitrile (MeCN–HZ), the deprotonated cluster interacting with methoxonium ions ($MeOH_2$–Z), and a deprotonated cluster interacting with ammonium ions (NH_4–Z). In addition, another EFG calculation was carried out with a methyl group replacing the Brønsted proton H1 in Fig. 1 (CH_3Z). These sites are called surface methoxy groups, and they play a crucial role in some catalytic cycles. Fig. 2 shows only the central parts of the clusters omitting the terminal $-Si(OH)_3$ fragments for the sake of clarity.

Note that NH_4^+ and $MeOH_2^+$ ions form two hydrogen bonds with two oxygen atoms of the AlO_4 tetrahedron (Fig. 2). Methanol accepts a hydrogen bond from the Brønsted proton and donates a second, weaker hydrogen bond to another oxygen atom of the AlO_4 tetrahedron [24–26]. In contrast, acetonitrile is a probe molecule which forms a relatively strong hydrogen bond to the Brønsted proton, but does not donate a hydrogen bond to a neighboring framework oxygen atom [27,28].

3. Results and discussion

3.1. Classification of geometries and bond perturbation effects

All structures were obtained by DFT optimisations of the clusters using model I. The final geometry of the zeolite cluster (HZ) is shown in Fig. 1 and corresponding interatomic distances and angles are listed in Table 1 for all clusters. The H1–Al distance in Fig. 1 is 246 pm which compares well with an experimental value of 248 pm reported by Fenzke, Hunger, and Pfeifer [29]. These authors determined the ^{1}H–^{27}Al distance for the Brønsted proton in the supercage of zeolite Y by analysing the heteronuclear dipole interaction from the spinning sideband pattern in the ^{1}H MAS NMR spectra.

If the oxygen atom O1 is protonated or methylated (HZ, CH_3Z, CH_3CN–HZ, MeOH–HZ), then the Al–O1 distance is longer than 188 pm (Table 1). If O1 or O2 are hydrogen bond acceptor atoms, then the corresponding Al–O1(O2) distance is between 172 and 185 pm (MeOH–HZ, $MeOH_2$–Z, NH_4–Z). Except for Z^-, the non-interacting oxygen atoms form Al–O bonds shorter than 172 pm. Z^- exhibits Al–O bonds which do not deviate by more than 0.7 pm from the average distance of 174.6 pm. All clusters show nearly the same value for the average Al–O distances in Table 1 (174.6–176.1 pm). These average Al–O distances are in good agreement with expected values from crystal structures of ordered tetrahedral framework aluminosilicates. Some insights can be obtained by comparing the geometries of HZ and Z^- in Table 1. Protonation of O1 in HZ reduces the bond strengths of O1 with Si and Al, and the corresponding distances are larger than in Z^-. The lengthening of the Al–O1 bond leads to a contraction of other bonds in the AlO_4 tetrahedra (Table 1); that is to say a perturbation on one bond is counterpoised by other bonds to result in approximately constant average Al–O distances.

Crystallographers often use empirical bond-length bond-valence relationships in order to scrutinize whether the bond-valence sum around an atom is equivalent to its valence. This is a method to discern the accuracy of the structure [30,31]. The Al–O bond-valence (s) for Al is calculated from the distance r with the empirical equation $s = \exp[(1.651 - r)/0.37]$. When this method is applied to the aluminium atoms in Table 1, then the sum of bond valences (empirical valences in Table 1) for Al are very close to the expected value of three. This result shows that the geometries listed in Table 1 withstand a test which is widely accepted among crystallographers. Additionally, the local geometries compare

Table 1
Distances (in pm) and angles (in degrees) in the optimized clusters, bond orders are given in parenthesis

	HZ	CH_3Z	CH_3CN–HZ	MeOH–HZ	$MeOH_2$–Z	NH_4–Z	Z^-
Classification	$O_3^nAlO^p$	$O_3^nAlO^p$	$O_3^nAlO^p$	$O_2^nAlO^pO^a$	$O_2^nAlO_2^a$	$O_2^nAlO_2^a$	O_4^nAl
Distance in pm (bond order)							
Al–O1	194.3	193.3	188.8	192.9	184.2	179.4	175.2
	(0.15)	(0.16)	(0.19)	(0.18)	(0.23)	(0.27)	(0.33)
Al–O2	170.4	170.6	171.7	172.4	181.5	177.9	173.9
	(0.39)	(0.37)	(0.36)	(0.34)	(0.27)	(0.28)	(0.35)
Al–O3	169.6	169.7	170.7	169.4	169.8	171.9	174.8
	(0.37)	(0.38)	(0.37)	(0.38)	(0.36)	(0.36)	(0.33)
Al–O4	168.9	169.7	169.9	169.2	168.9	170.8	174.4
	(0.39)	(0.39)	(0.39)	(0.39)	(0.39)	(0.38)	(0.34)
avg. Al–O distance	175.8	175.8	175.3	176.0	176.1	175.0	174.6
O1–H1	97.1	149.1[a]	103.3	107.1	142.9	167.2	–
	(0.30)	(0.18)[a]	(0.21)	(0.19)	(0.11)	(0.08)	
Si1–O1	168.0	168.0	166.0	167.3	163.3	161.8	158.3
	(0.26)	(0.27)	(0.28)	(0.29)	(0.31)	(0.33)	(0.40)
Σ bond orders O1	0.71	0.61	0.65	0.66	0.65	0.68	0.73
bond orders Al	1.30	1.30	1.31	1.29	1.25	1.29	1.35
'empirical valence of Al' (see text)	3.11	3.10	3.10	3.08	3.02	3.08	3.10
Angles in degrees							
O1–Al–O2	97.3	99.1	100.0	97.2	97.2	101.8	110.0
O1–Al–O3	105.0	107.6	107.8	108.0	106.1	111.0	112.5
O1–Al–O4	103.7	103.7	106.2	102.9	106.7	112.4	109.9
O2–Al–O3	115.2	114.1	112.7	114.6	112.5	106.5	106.1
O2–Al–O4	116.4	115.0	115.2	115.6	116.1	112.3	110.8
O3–Al–O4	115.6	115.0	113.5	115.7	115.7	112.3	107.5

[a]Values for O–C bond instead of O–H.

well with quantum-chemical results from other groups [12], and the constant average Al–O bond lengths have been observed before [32].

This total valence stability against such severe perturbations as the protonation of oxygen atoms in zeolite frameworks corresponds to the well-known bond-order conservation principle in quantum-chemical calculations [13]. The bond order is defined as the number of electrons in the bonding orbitals between two atoms divided by two (if no antibonding orbitals are occupied). Bond orders as obtained by the DFT calculations are listed in parenthesis in Table 1. Quantum-chemical bond orders depend on the basis set, but for the constant basis set 6-31G** the bond order conservation rule holds rather well as the sum of bond orders for O1 and Al is nearly the same for all clusters in Table 1.

Other conspicuous structural details are given by the O–Al–O angles in Table 1. For all structures but Z^- the O1–Al–O2 angles are by at least 7° smaller than the tetrahedral angle. This result is easily rationalized by the perturbation on this side of the tetrahedra except for Z^-. Even more interesting are the large values for the angles O2–Al–O3, O2–Al–O4, and O3–Al–O4 when O1 is protonated. In this case, these values are closer to 120° than to 109.5°. In conjunction with the long Al–O1 distance, this observation means that the Al atom is not in a real tetrahedral coordination if O1 is protonated. Instead, the AlO_4 site shows a structure which is in between a tetrahedral geometry and a trigonal planar coordination (see also Fig. 1). This observation is corroborated by the bond orders which show about half the value for Al–O1, when O1 is protonated, as compared to the other Al–O bonds (Table 1). All these observations are consistent with a model of the acid site as an SiOH group promoted by the neighboring Lewis acidic framework aluminium atom [13]. The quadrupole interaction in ^{27}Al NMR could be a potential parameter to probe the electronic Al–O bond

strain in zeolitic acid sites. This conjecture is further pursued below.

From the geometric and bonding properties the clusters of Table 1 are classified according to three different types of oxygen atoms surrounding the aluminium atom: a protonated or methylated oxygen atom (O^p), a hydrogen bond accepting oxygen atom (O^a), and a non-perturbed oxygen atom (O^n). According to this designation MeOH–HZ is of type $O_2^nAlO^pO^a$ and so on (Table 1).

3.2. EFG orientation

The orientation of the principal components V_{xx}, V_{yy}, and V_{zz} of the EFG tensor is shown in Fig. 1 for HZ. V_{zz} is nearly parallel to the O1–Al direction and the O1–Al–V_{zz} angle is 176.4°. The O1–Al–V_{zz} angles are listed for all clusters in Table 2. This angle does not deviate by more than 7° from 180° in Table 2, when O1 is of type O^p (HZ, MeOH–HZ, MeCN–HZ), or when a methyl group is substituted for the Brønsted proton (CH_3–Z). This observation shows that an Al–O^p bond determines the orientation of V_{zz}. When the two oxygen atoms O1 and O2 are of type O^a ($MeOH_2$–Z, NH_4–Z), then the O1–Al–V_{zz} angles are close to 90° in Table 2, and the V_{zz} vector is about perpendicular to the O1–Al–O2 plane. In this situation the orientation of V_{zz} is not directed along a single Al–O bond. Instead, two equivalently perturbed Al–O^a bonds are now to be considered. The orientation of the EFG tensor is not specific for Z^-. The EFG orientation corresponds to the local symmetry and it appears to be largely a function of the presence of O^p, O^a, and O^n oxygen atoms. It is concluded that quadrupole interaction for ^{27}Al in zeolites is mainly a local effect of the AlO_4 tetrahedra.

3.3. Effects of basis sets and cluster sizes in model I

The QCC for ^{27}Al in HZ as calculated with model I is 18.2 MHz and the asymmetry parameter (η) is 0.15 when the 6-31G** basis set is used. Single-point calculations on the same geometry with the smaller 3-21G** basis set yields QCC = 14.9 MHz ($\eta = 0.21$) and the larger 6-311G** results in a QCC value of 21.8 MHz ($\eta = 0.16$). Full geometric optimisations of small molecules ($AlCl_3$, $(HO)_3AlOH_2$) with various basis sets and quantum-chemical methods (DFT and SCF/MP2) confirm that QCC becomes larger upon increasing the size of the mentioned Pople basis sets. The observed variations of QCC are not due to the density functional method.

The basis set in model I does not alter the orientation of the EFG significantly. Additionally, the asymmetry parameter shows only a minor dependence on the basis set, and it has obviously converged to a stable value for basis sets larger than 3-21G**. These observations clearly show that the different EFG components are in the right relative scale to each other, but the absolute values are dependent on the basis sets. This scaling is eliminated in a relative EFG property like the asymmetry parameter (Eq. (2)) as opposed to the absolute EFG quantity QCC (Eq. (1)) which depends on the size of V_{zz}.

Calculations of different cluster sizes show that an increase of the cluster size would not improve the results of the EFG calculations. This result was

Table 2
Quadrupole interaction parameters obtained from models I–III compared with experimental values

Model	Parameter	H–Z	CH_3Z	CH_3CN–HZ	MeOH–Z	$MeOH_2$–Z	NH_4–Z	Z^-
I	QCC/MHz	18.2	16.2	13.5	15.5	−8.2	−6.6	−2.0
	η	0.15	0.16	0.26	0.30	0.85	0.73	0.61
	O1–Al–V_{zz}	176.4	175.9	175.3	173.3	88.2	93.6	128.6
II	QCC/MHz	−1.2	−0.9	−0.84	−1.0	−0.4	−0.3	0.3
	η	0.14	0.18	0.13	0.14	0.35	0.36	0.34
III	QCC/MHz	7.3	6.1	4.6	6.0	4.4	3.5	1.6
exp.	QCC	11–18	–	–	5–7[b]	5–10	0–5[a]	

[a]Crudely estimated range for fully hydrated zeolites.
[b]Assignment to MeOH–Z or $MeOH_2$–Z not trivial, since dynamic effects are important (see text).

achieved by using the differently sized protonated clusters shell-1, shell-1.5, shell-2, and the faujasite model in Ref. [25]. These geometries were kindly provided by Haase and Sauer, who used ab initio calculations including electron correlation for optimising the structures.

3.4. Models I–III and comparison with experimental values

Table 2 lists the QCC and asymmetry parameters of the EFGs for models I–III and the experimental values known from literature. It is striking that all clusters with an oxygen atom of type O^p (HZ, CH_3Z, MeOH–HZ, MeCN–HZ) show a large QCC value (13.5–18.2 MHz). For cases with two O^n and two O^a oxygen atoms ($MeOH_2$–Z, NH_4–Z) QCC shows an intermediate value with negative sign (−8.2 and −6.6 MHz, respectively). For four O^n atoms around the aluminium atom (Z^-) the magnitude of QCC is small (2 MHz).

Since the size and orientation of V_{zz} are obviously a function of bond distortion effects, the computed Al–O bond orders are used for a correlation between bond properties and the QCC (Fig. 3). This is to demonstrate the importance of bond effects as to the size of the QCC. Such a correlation must take into account the different bonding situations. To this end, three different classes of perturbations of the AlO_4 tetrahedra are distinguished. Protonation of the framework is a large perturbation where the z-direction of V_{zz} is dominated by the Al–O^p bonds, and this bond order is taken accordingly for the analysis of cases with O^p. If two O^a atoms are present, which corresponds to a medium perturbation on two oxygen atoms, then the average of the two Al–O^a bond orders is used. For O_4^nAl, the non-distorted, or more generally the uniformly perturbed AlO_4 site, the average of all four Al–O^n bond orders is used. The choice of different numbers of bonds which enter the correlation can be understood on the basis of approximate local symmetry considerations. Due to the dominance of O^p, O_3AlO^p and $O_2O^aAlO^p$ are of C_{3v}-like symmetry for the EFG. $O_2AlO_2^a$ is of C_{2v}-like local symmetry with two similar O^a atoms. AlO_4^n is of T_d-like symmetry. The number of Al–O bonds entering the correlation is determined by these approximate local symmetries.

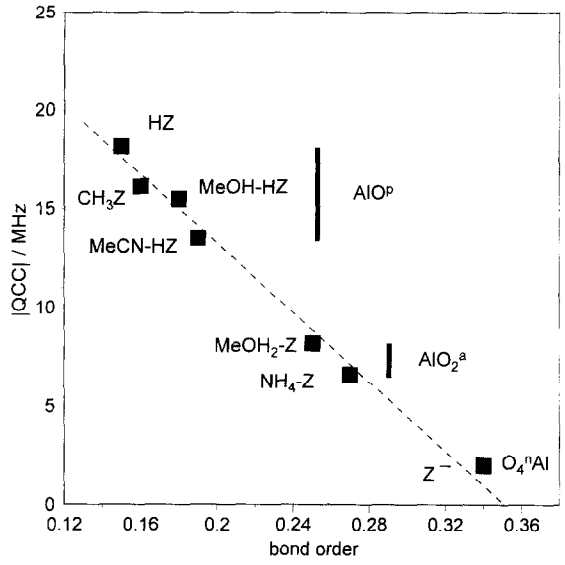

Fig. 3. Correlation between the magnitude of the calculated quadrupole coupling constant (QCC) and Al–O bond orders of the perturbed oxygen atoms (see text); the AlO^p region includes data where only the Al–O1 bond order is considered, AlO_2^a includes data with the average of Al–O1 and Al–O2 bond orders, and for O_4^nAl the average of all four Al–O bond orders is used.

Fig. 3 shows a correlation between the magnitude of the calculated QCC and the Al–O bond orders corresponding to the three perturbation cases. A linear correlation is observed which holds for of all three cases. The smaller the bond order in Fig. 3, which means stronger perturbation, the larger is the QCC calculated with model I. The interaction between the Brønsted proton and a basic molecule decreases the O1–H1 bond order. The oxygen atom retains its valence by strengthening the bonds to Al and Si1, and the increased Al–O bond order results in a smaller QCC for ^{27}Al. Thus, the decrease of the QCC value is a function of the strength of the acid–base interaction. It is anticipated that acetonitrile could be a suitable probe molecule to study the zeolite acid strength by ^{27}Al NMR due to the clear decrease of QCC upon MeCN adsorption, and because an intricating proton exchange can not occur as for MeOH (vide infra).

Models II and III predict qualitatively the same trend as model I for the QCC in Table 2. However, the predicted differences are smaller. A comparison between the known experimental values [5–8] and

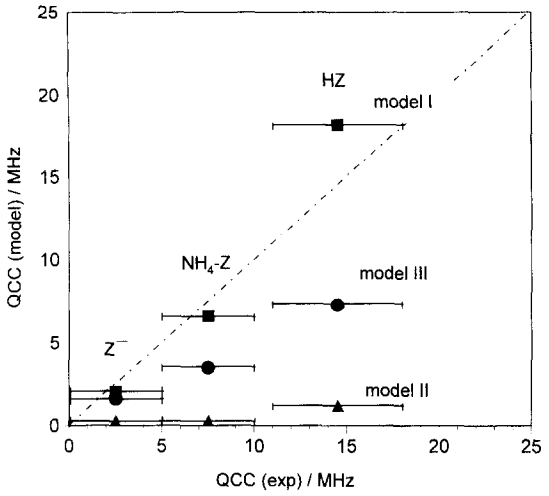

Fig. 4. Comparison between experimental quadrupole coupling constants (QCC) and predicted numbers from the three models; squares stand for model I, triangles for model II, and circles for model III; horizontal bars are not error bars but indicate experimental ranges from several sources.

the predictions of QCC from the three models is shown in Fig. 4. Since no experimental value is known for Z^-, we used an estimated range between 0 and 5 MHz. Results of this order of magnitude are typical for fully hydrated zeolites in the sodium form where only weak interactions between the framework oxygen atoms and Na^+ or H_2O exist. In addition, all four oxygen atoms of the AlO_4 tetrahedra are perturbed uniformly which preserves a symmetric case for hydrated zeolites in the sodium forms.

It is obvious that model I predicts the trends in the QCC best in agreement with experimental values in Fig. 4. Model II can be considered as a purely ionic model which does not take into account chemical bonds. This neglect of chemical bonds is most probably the reason why this method fails to predict reasonably the QCC of ^{27}Al in zeolites. Model III is an empirical method which has been established for many structures other than acidic zeolites. This method places emphasis on geometrical strain. Geometrical factors are obviously not a sufficient explanation for the large QCC values of ^{27}Al for zeolites with protonated oxygen atoms, since model III also predicts too small values. The severe perturbation concentrated on one oxygen atom of the AlO_4 tetrahedron does not occur in the structures for which model III has been developed and applied so far [10,11,33]. These observations clearly show the importance of the electronic bond strain as a dominating factor for the EFG at aluminium in acidic zeolites. This effect of bond strain is illustrated in the correlation of QCC with the bond order in Fig. 3. Experimental asymmetry parameters are less reliable than the QCC. The difficulties at evaluating the uniqueness of a set of line simulation parameters can obscure the experimental asymmetry parameter more dramatically than the QCC values [8]. However, a general trend of experimental values of η seems to meet with the results of model I here: for C_{3v}-like symmetry (O_3AlO^p, $O_2O^aAlO^p$) the asymmetry parameter is small (< 0.5), and for C_{2v}-like symmetry ($O_2AlO_2^a$) η is large (> 0.5).

MeOH–HZ and $MeOH_2$–Z deserve special attention due to the contemporary issue as to whether methanol is protonated in zeolites or not [24–26,34]. This question is crucial for understanding the mechanism of the technically important methanol-to-gasoline reaction in zeolites [35,36]. From Table 2, it could be concluded that ^{27}Al NMR spectroscopy is a very straightforward method to distinguish between the two scenarios MeOH–HZ and $MeOH_2$–Z. An experimental range for the QCC of ^{27}Al between 5–7 MHz has been published by Hunger and Horvath [9] for HZSM-5 loaded with one molecule methanol per acid site. This observation would apparently suggest that protonation of methanol has taken place. However, such a biased conclusion would not take into account a fast proton exchange between unprotonated methanol and the zeolitic proton according to the reaction O1–H′O(Me)H″O2 ⇄ O1H′(Me)OH″–O2. This process occurs even at low temperatures due to the small activation barrier of ca. 10 kJ/mol [24,25]. Such a proton exchange would average the Al–O1 and Al–O2 bonds for MeOH–HZ, and the averaged bond order has to be taken for a prediction of QCC using the correlation shown in Fig. 3. The averaged bond order is 0.26 which is very close to the two bond orders Al–O1 (0.23) and Al–O2 (0.27) for $MeOH_2$–Z (Table 1). To verify this result a number of EFG calculations have been carried out over the reaction coordinate of the proton exchange using the DFT. Only the positions of the most important atoms (Al, O1, O2, H1, $H_{methanol}$) were varied for CPU time reasons. Calculating the averaged EFG

components and diagonalising the obtained tensor gives indeed dynamically averaged values for MeOH–HZ which are very close to those of the rigid $MeOH_2$–Z. This result means that ^{27}Al NMR can not distinguish between $MeOH_2$–Z and MeOH–HZ considering the aforementioned dynamical exchange.

4. Conclusions

The QCC of ^{27}Al in zeolite correlates with the Al–O bond perturbation in the AlO_4 tetrahedra. For zeolitic acid sites the chemical bonds dominate the EFG at the aluminium centers, while geometric factors and ionic charges play a less important role. These conclusions arise from the empirical shear strain parameter (model III) and from the point charge model (model II) predicting too small QCC. Due to the severe bond perturbation, the presence of a Brønsted proton causes a large QCC which decreases upon interaction of the proton with a base. The extent of the decrease depends on the nature of the base, and, presumably, on the strength of the acid site. The observed trends, when different bases are adsorbed in a certain zeolite, could be a valuable means to a deeper understanding of the Brønsted site. Acetonitrile could be a useful candidate as a probe molecule while methanol adsorption is too complicated due to a dynamic proton exchange. However, based on the results here, a general correspondence between the intrinsic acidity of different zeolites in their H-forms and the ^{27}Al QCC can not be predicted.

Acknowledgements

The work was funded by the European Union under contract ERBCHBGCT930309. A budget on a Cray C98-YMP supercomputer was financed by the Stichting Nationale Computer Faciliteiten of the Netherlands under project SC-451. Continuous discussions with M. Hunger (University of Stuttgart/Germany) are gratefully acknowledged, who also made available to us some experimental results prior to publication. The structures for testing the influence of cluster sizes were taken from Ref. [25], and we thank F. Haase and J. Sauer for providing the atomic coordinates.

References

[1] P.B. Weisz, V.J. Frilett, J. Phys. Chem. 64 (1960) 382.
[2] A. Corma, Chem. Rev. 95 (1995) 559.
[3] N.Y. Chen, W.E. Garwood, F.G. Dwyer, Shape Selective Catalysis in Industrial Applications. Marcel Dekker, New York, 1989.
[4] P.R. Pujadó, J.A. Rabó, G.J. Antos, S.A. Gembicki, Catal. Today 13 (1992) 113.
[5] H. Ernst, D. Freude, I. Wolf, Chem. Phys. Lett. 212 (1993) 588.
[6] M. Hunger, T. Horvath, G. Engelhardt, H.G. Karge, Stud. Surf. Sci. Catal. 94 (1995) 756.
[7] D. Freude, J. Haase, NMR—Basic Principles and Progress 29 (1993) 1.
[8] C.P. Grey, A.J. Vega, J. Am. Chem. Soc. 117 (1995) 8232.
[9] M. Hunger, T. Horvath, Ber. Bunsenges. Phys. Chem. 99 (1995) 1316.
[10] G. Engelhardt, W. Veeman, J. Chem. Soc. Chem. Commun. (1993) 622.
[11] S. Ghose, T. Tsang, Amer. Mineral. 58 (1973) 748.
[12] J. Sauer, P. Ugliengo, E. Garrone, V.R. Saunders, Chem. Rev. 94 (1994) 2095.
[13] R.A. van Santen, G.J. Kramer, Chem. Rev. 95 (1995) 637.
[14] E.A.C. Lucken, Nuclear Quadrupole Coupling Constants, Academic Press, London, 1969.
[15] E.R. Davidson, D. Feller, Chem. Rev. 86 (1986) 681.
[16] M.H. Palmer, J.A. Blair-Fish, Z. Naturforsch. 49a (1994) 137.
[17] B.A. Huggins, P.D. Ellis, J. Am. Chem. Soc. 114 (1992) 2098.
[18] M.J. Frisch, G.W. Trucks, H.B. Schlegel, P.M.W. Gill, B.G. Johnson, M.W. Wong, J.B. Foresman, M.A. Robb, M. Head-Gordon, E.S. Replogle, R. Gomperts, J.L. Andres, K. Raghavachari, J.S. Binkley, C. Gonzalez, R.L. Martin, D.J. Fox, D.J. Defrees, J. Baker, J.J.P. Stewart, J.A. Pople, Gaussian 92/DFT, Revision G.4, Gaussian, Pittsburgh, PA, 1993.
[19] R.G. Parr, W. Yang, Density-Functional Theory of Atoms and Molecules, Oxford University Press, Oxford, 1989.
[20] M. Czjzek, H. Jobic, A.N. Fitch, T. Vogt, J. Phys. Chem. 96 (1992) 1535.
[21] B.G. Johnson, P.M.W. Gill, J.A. Pople, D.J. Fox, Chem. Phys. Lett. 206 (1993) 239.
[22] D. Sundholm, J. Olsen, Phys. Rev. Lett. 68 (1992) 927.
[23] H. Koller, G. Engelhardt, A.P.M. Kentgens, J. Sauer, J. Phys. Chem. 98 (1994) 1544.
[24] S.R. Blaszkowski, R.A. van Santen, J. Phys. Chem. 99 (1995) 11728.
[25] F. Haase, J. Sauer, J. Am. Chem. Soc. 117 (1995) 3780.
[26] S. Bates, J. Dwyer, J. Molec. Struct. (Theochem) 306 (1994) 57.

[27] J.F. Haw, M.B. Hall, A.E. Avarado-Swaisgood, E.J. Munson, Z. Lin, L.W. Beck, T. Howard, J. Am. Chem. Soc. 116 (1994) 7308.
[28] E.L. Meijer, R.A. van Santen, A.P.J. Jansen, J. Phys. Chem. 100 (1996) 9282.
[29] D. Fenzke, M. Hunger, H. Pfeifer, J. Magn. Reson. 95 (1991) 477.
[30] I.D. Brown, in: M. O'Keefe, A. Navrotsky (Eds.), Structure and Bonding, Vol. II, 1980, p. 1.
[31] I.D. Brown, D. Altermatt, Acta Crystallogr. B41 (1985) 244.
[32] J. Sauer, C.M. Kölmel, J.-R. Hill, R. Ahlrichs, Chem. Phys. Lett. 164 (1989) 193.
[33] G. Engelhardt, H. Koller, P. Sieger, W. Depmeier, A. Samoson, Solid State NMR 1 (1992) 127.
[34] R. Shah, M.C. Payne, M.-H. Lee, J.D. Gale, Science 271 (1996) 1395.
[35] S.R. Blaszkowski, M.A.C. Nascimento, R.A. van Santen, J. Phys. Chem. 100 (1996) 3463.
[36] P.E. Sinclair, C.R.A. Catlow, J. Chem. Soc. Faraday Trans. 92 (1996) 2099.